european journal
of neurology
the official journal of the european academy of neurology

ORIGINAL ARTICLE

Paramagnetic rim lesions are associated with inner retinal layer thinning and progression independent of relapse activity in multiple sclerosis

Nik Krajnc[1,2] | Leo Hofer[2,3] | Fabian Föttinger[1,2] | Assunta Dal-Bianco[1,2] | Fritz Leutmezer[1,2] | Barbara Kornek[1,2] | Paulus Rommer[1,2] | Gregor Kasprian[2,3] | Thomas Berger[1,2] | Berthold Pemp[4] | Lukas Haider[2,3] | Gabriel Bsteh[1,2]

[1]Department of Neurology, Medical University of Vienna, Vienna, Austria

[2]Comprehensive Center for Clinical Neurosciences and Mental Health, Medical University of Vienna, Vienna, Austria

[3]Biomedical Imaging and Image-Guided Therapy, Medical University of Vienna, Vienna, Austria

[4]Department of Ophthalmology, Medical University of Vienna, Vienna, Austria

Correspondence
Gabriel Bsteh, Department of Neurology, Medical University of Vienna, Waehringer Guertel 18-20, 1090 Vienna, Austria.
Email: gabriel.bsteh@meduniwien.ac.at

Abstract

Background and purpose: Paramagnetic rim lesions (PRLs) are chronic active lesions associated with a severe disease course in multiple sclerosis (MS). This study was undertaken to investigate an association between retinal layer thinning (annualized loss of peripapillary retinal nerve fiber layer [aLpRNFL] and ganglion cell–inner plexiform layer [aLGCIPL]) and PRLs in patients with MS (pwMS).

Methods: In this study, pwMS with brain magnetic resonance imaging and ≥2 optical coherence tomography scans were included. Cox proportional hazard regression models were performed using progression independent of relapse activity (PIRA) as the dependent variable, and aLpRNFL, aLGCIPL, or the number of PRLs as independent variables, adjusted for covariates.

Results: We analyzed data from 97 pwMS (mean age = 35.2 years [SD = 9.9], 71.1% female, median disease duration = 2.3 years [interquartile range = 0.9–9.0]). The number of PRLs was associated with aLpRNFL and aLGCIPL. PIRA was observed in 18 (18.6%) pwMS, with aLpRNFL (hazard ratio [HR] = 1.44 per %/year), aLGCIPL (HR = 1.61 per %/year), and the number of PRLs (HR = 1.24 per PRL) being associated with increased risk of PIRA.

Conclusions: The number of PRLs is associated with inner retinal layer thinning and increased risk of PIRA. A combination of PRLs and retinal layer thinning could serve as a surrogate for pwMS at highest risk of disability progression.

KEYWORDS
GCIPL, iron rim, multiple sclerosis, PIRA, pRNFL

INTRODUCTION

Multiple sclerosis (MS) is a chronic inflammatory disease of the central nervous system (CNS) with features of acute demyelinating as well as chronic active inflammation in the white and grey matter. In contrast to active demyelinating lesions with blood–brain barrier impairment, chronic active lesions are characterized by proinflammatory microglia/macrophages at their edges that accumulate iron

Lukas Haider and Gabriel Bsteh contributed equally and share last authorship.

[1, 2]. These lesions can be visualized as so-called paramagnetic rim lesions (PRLs) by iron-sensitive magnetic resonance imaging (MRI), that is, susceptibility-weighted imaging (SWI) or quantitative susceptibility mapping [3]. PRLs occur in up to 60% of patients with MS (pwMS), reaching their highest prevalence in late relapsing–remitting MS [4]. Although the exact pathophysiological mechanism contributing to their development remains unclear [5], PRLs are associated with a profound axonal transection, as reflected by prolonged intra- and perilesional T1 relaxation times [6–8], and also with progression independent of relapse activity (PIRA) [9], a critical determinant of disability accumulation driving long-term prognosis in MS.

Inner retinal layer thinning, as measured by optical coherence tomography (OCT), is an emerging biomarker of neuroaxonal damage in MS [10]. Peripapillary retinal nerve fiber layer (pRNFL) and ganglion cell–inner plexiform layer (GCIPL) thickness are both robust indicators of neuroaxonal degeneration in MS [11], and their thinning is associated with an increased risk of disability progression including PIRA [12–15]. Recently, we reported a cross-sectional association of the number of PRLs with pRNFL and GCIPL thickness [16], indicating that PRL load transfers to more pronounced neuroaxonal damage as reflected by OCT.

Here, we aimed to investigate whether the number of PRLs is also associated with longitudinal degree of inner retinal layer thinning in MS.

METHODS

Patients and definitions

For this longitudinal retrospective study, patients from the Vienna MS database (VMSD) were included based on following inclusion criteria: (i) relapsing onset MS diagnosis according to the 2017 version of the McDonald criteria [17]; (ii) age ≥ 18 years; (iii) availability of T1-, fluid-attenuated inversion recovery (FLAIR)-, and SWI-based MRI scan at 3 T; and (iv) availability of an OCT scan <90 days from MRI and at least one follow-up OCT scan ≥12 months later [18]. To avoid effects of treatment change on retinal layer thinning, we included only patients without disease-modifying therapy (DMT) change within 3 months before baseline and during follow-up [19]. The selection process based on the inclusion and exclusion criteria is shown in Figure 1. Data on Expanded Disability Status Scale (EDSS) and relapses were obtained at the time of MRI and at every clinical visit at 3- or 6-month intervals for up to 5 years [20]. A relapse was defined as patient-reported symptoms and objectively confirmed neurological signs typical of an acute CNS inflammatory demyelinating event with duration of at least 24 h in the absence of fever or infection and separated from the last relapse by at least 30 days [21]. Relapses were further classified as either resulting or not resulting in a subsequent EDSS worsening sustained 6 months after relapse (relapse-associated worsening) compared to the last EDSS before the relapse. PIRA was
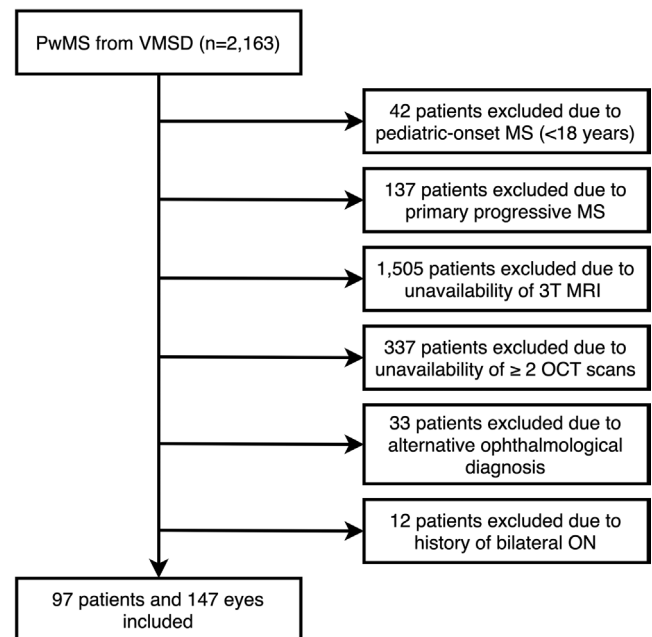
FIGURE 1 Flowchart of patients' selection based on the inclusion and exclusion criteria. MRI, magnetic resonance imaging; MS, multiple sclerosis; OCT, optical coherence tomography; ON, optic neuritis; PwMS, patients with MS; VMSD, Vienna MS database.

defined as a confirmed EDSS increase (≥1.5/1.0/0.5 points from baseline score of 0/1.0–5.5/≥6.0 points) with no clinical attack in the 30 days before or after the EDSS increase and confirmed after 6 months [22, 23].

The patients' DMT status was classified as follows: (i) "no DMT," defined as patients receiving no DMT; (ii) "moderately effective DMT (M-DMT)," defined as patients receiving either interferon-beta preparations, glatiramer acetate, dimethyl fumarate, or teriflunomide; or (iii) "highly effective DMT (H-DMT)," defined as patients receiving either natalizumab, fingolimod, siponimod, ponesimod, ozanimod, alemtuzumab, cladribine, ocrelizumab, ofatumumab, or rituximab.

Optical coherence tomography

OCT imaging was performed by experienced neuro-ophthalmologists at the Department of Ophthalmology and Optometry using the same spectral-domain OCT (Spectralis OCT, Heidelberg Engineering, Heidelberg, Germany; Heidelberg eye explorer software version 5.4.8.0) without pupil dilatation in a dark room on both eyes of each patient. For pRNFL measurement, a custom 12° (3.4 mm) ring scan centered on the optic nerve head was used (1536 A-scans, automatic real-time tracking [ART]: 100 averaged frames) [24]. For GCIPL measurement, a 20° × 20° macular volume scan (512 A-scans, 25 B-scans, vertical alignment, ART: 16 averaged frames) centered on the macula was performed. GCIPL thickness was defined as the mean layer thickness of the

four inner and outer quadrants of the circular grid centered around the foveola corresponding to the 3- and 6-mm rings as defined by the Early Treatment Diabetic Retinopathy Study [25]. Image processing was conducted semiautomatically using the built-in proprietary software with manual correction of obvious errors. All examinations were checked for sufficient quality using OSCAR-IB criteria [26]. OCT scans that lacked macula scan or did not fulfill OSCAR-IB criteria were excluded from the final analysis.

Thicknesses of GCIPL and pRNFL were calculated as the mean of the values for both eyes. Patients with a history of unilateral optic neuritis (ON) <6 months before baseline were excluded from the study. Eyes with a history of ON ≥6 months before baseline were eligible for inclusion. Eyes suffering ON during the observation period were excluded from the study, and only the values of eyes without ON during the observation period were used for calculation of retinal thinning in the analyses. To identify subclinical ON during the course of the study, we used interocular asymmetry with cutoff values of ≥5 μm for pRNFL and ≥4 μm for GCIPL [27, 28]. In these cases, we used only the eye with the higher value. In this way, all parameters used for statistical analyses are not underlying intereye interactions. Annualized loss of pRNFL and GCIPL (aLpRNFL, aLGCIPL) was calculated by individual linear regression models as the slope of the regression line best fitted to all measurements over the observation period. Patients with diagnoses of ophthalmologic (i.e., myopia greater than −4 diopters, optic disc drusen, glaucoma), neurologic, or drug-related causes of retinal damage not attributable to MS were excluded [29]. All patients were screened for the presence of macular edema and excluded if macular edema occurred. The investigators performing the OCT were blinded to clinical parameters and vice versa. The quantitative OCT study results were reported using the revised Advised Protocol for OCT Study Terminology and Elements (APOSTEL 2.0) recommendations [30].

MRI acquisition

All cranial MRI scans between January 2015 and December 2023 were performed on a Siemens (Erlangen, Germany) Magnetom 3-T MRI system, using a 64-channel radio frequency coil. Isovoxel (1 mm^3) three-dimensional FLAIR (repetition time [TR] = 6000 ms, echo time [TE] = 288 ms, inversion time [TI] = 2100 ms), T1-weighted images (TE = 2,16 ms, TR = 1670 ms, flip angle = 15°; before and after gadolinium [Gd]-based contrast administration), and SWI sequences (TE = 40 ms, TR = 49 ms, image matrix = 224 × 256, slices = 80, slice thickness = 2 mm) were acquired consecutively.

Evaluation of MRI lesions

Periventricular, juxtacortical, deep white matter, and infratentorial lesions were analyzed by two raters experienced in MS imaging in consensus (L.Ho., L.Ha.). PRLs were defined as FLAIR-hyperintense lesions that were partially or completely surrounded by a pronounced and distinct SWI-hypointense rim. Gd-enhancing lesions were excluded from the analysis. Patients were grouped according to the number of PRLs (0 PRLs, 1–3 PRLs, and ≥4 PRLs) [31].

Standard protocol approvals, registrations, patient consents, and reporting

The study was approved by the ethics committee of the Medical University of Vienna (ethical approval number: 1257/2022). Because this was a retrospective study, the requirement for written informed consent from study participants was waived by the ethics committee. This study adheres to the reporting guidelines outlined within the STROBE (Strengthening the Reporting of Observational Studies in Epidemiology) Statement.

Statistics

Statistical analysis was performed using SPSS 26.0 (SPSS, Chicago, IL, USA). Categorical variables are expressed in frequencies and percentages, and continuous variables as mean and SD or median and interquartile range (IQR) as appropriate. Continuous variables were tested for normal distribution by the Kolmogorov–Smirnov test with Lilliefors correction.

Multivariate linear stepwise regression models were fitted with OCT parameters (aLpRNFL, aLGCIPL) as dependent variables and the number of PRLs as an independent variable, adjusted for age, sex, disease duration, EDSS at baseline, DMT group, T2 lesion count, and visual pathway lesion count. Multivariate Cox proportional hazard regression models were performed using PIRA as the dependent variable and aLpRNFL, aLGCIPL, or the number of PRLs as independent variables, adjusted for age, sex, disease duration, EDSS at baseline, DMT group, T2 lesion count, and visual pathway lesion count.

Regression models were checked for collinearity by variance inflation factor (VIF) excluding all variables if the VIF was >2.0, corresponding to an R^2 of 0.50. Missing values were handled by multiple (20 times) imputation using the missing not at random approach with pooling of estimates according to Rubin's rules [32].

Prespecified sensitivity analyses to determine the potential confounding influence were performed with the same statistical analysis setup excluding patients with secondary progressive MS (SPMS).

The significance level was set at a two-sided p-value <0.05. All multiple analyses were corrected using the Bonferroni method.

RESULTS

In all, 97 pwMS were included (mean age = 35.2 years [SD = 9.9], 71.1% female, median disease duration = 2.3 years [IQR = 0.9–9.0],

TABLE 1 Characteristics of the study cohort at baseline.

Characteristic	Study cohort, $n = 97$
Demographics and clinical characteristics	
Female[a]	69 (71.1)
Age, years[b]	35.2 (9.9)
Disease duration, years[c]	2.3 (0.9–9.0)
EDSS[c]	2.0 (0–3.0)
RRMS[a]	89 (91.8)
History of unilateral ON[a]	50 (51.5)
DMT	
Time on DMT at baseline, months[c]	5 (3–14)
No DMT[a]	8 (8.2)
M-DMT[a]	42 (43.3)
Interferon-beta preparations	7 (7.2)
Glatiramer acetate	10 (10.3)
Dimethyl fumarate	21 (21.6)
Teriflunomide	4 (4.1)
H-DMT[a]	47 (48.5)
S1PM	15 (15.5)
Cladribine	15 (15.5)
Natalizumab	5 (5.2)
Anti-CD20 mAbs	12 (12.4)
MRI data	
Presence of PRLs[a]	55 (56.7)
Number of PRLs[d]	1 (0–10)
T2 lesion count[c]	18 (10–39)
Visual pathway lesion count[c]	3 (1–5)
OCT data	
Time from MRI to OCT, days[d]	75 (0–90)
pRNFL, μm[b]	96.4 (11.4)
GCIPL, μm[b]	67.4 (6.0)

Abbreviations: Anti-CD20 mAbs, monoclonal antibodies against cluster of differentiation 20; DMT, disease-modifying therapy, EDSS, Expanded Disability Status Scale; GCIPL, ganglion cell–inner plexiform layer; H-DMT, highly effective DMT; M-DMT, moderately effective DMT; MRI, magnetic resonance imaging; OCT, optical coherence tomography; ON, optic neuritis; PRL, paramagnetic rim lesion; pRNFL, peripapillary retinal nerve fiber layer; RRMS, relapsing–remitting multiple sclerosis; S1PM, sphingosine-1-phosphate receptor modulator.

[a]n (%).
[b]Mean (SD).
[c]Median (interquartile range).
[d]Median (range).

median EDSS = 2.0 [IQR = 0–3.0]). Median number of PRLs was 1 (range = 0–10), with 42 (43.3%), 46 (47.4%), and 9 (9.3%) pwMS having 0 PRLs, 1–3 PRLs, and ≥4 PRLs, respectively. Median number of OCT scans was 3 (range = 2–6) over a median follow-up time of 1.4 years (IQR = 1.0–2.1), with 52 (53.6%) patients having ≥3 OCT scans. Characteristics of the study cohort are shown in Table 1.

Inner retinal layer thinning

Mean aLpRNFL and aLGCIPL were −0.60%/year (SD = 1.50) and −0.50%/year (SD = 1.08), respectively. pwMS with PRLs had significantly higher aLpRNFL (−1.23%/year [SD = 1.42] vs. 0.09%/year [SD = 1.25], $p < 0.001$) and aLGCIPL (−0.88%/year [SD = 1.20] vs. −0.07%/year [SD = 0.72], $p < 0.001$) compared to pwMS without PRLs. In a multivariate linear regression model, aLpRNFL was associated with the number of PRLs ($\beta = -0.36$, 95% confidence interval [CI] = −0.32 to −0.26, $p < 0.001$), explaining 10.0% of its variance (Table 2, Figure 2). Similarly, aLGCIPL was associated with the number of PRLs ($\beta = -0.50$, 95% CI = −0.31 to −0.27, $p < 0.001$), explaining 29.3% of its variance (Table 2, Figure 2).

Progression independent of relapse activity

During a median interval of 24.5 (range = 12–85) months from baseline to the last follow-up, PIRA was observed in 18 (18.6%) pwMS. Patients with PIRA were older and had higher EDSS at baseline (Table S1). In the regression model, retinal layer thinning (aLpRNFL: hazard ratio [HR] = 1.44 per %/year, 95% CI = 1.34–1.56, $p < 0.001$; aLGCIPL: HR = 1.61 per %/year, 95% CI = 1.47–1.77, $p < 0.001$) and the number of PRLs (HR 1.24 per PRL, 95% CI = 1.17–1.32, $p < 0.001$) were both associated with an increased risk of PIRA. In a combination with ≥4 PRLs, aLpRNFL ≥ 1.0%/year (HR = 4.70, 95% CI = 3.51–6.29, $p < 0.001$) and aLGCIPL ≥ 1.0%/year (HR = 8.06, 95% CI = 6.11–10.64, $p < 0.001$) were associated with an approximately five- and eightfold increased risk of PIRA, respectively (Table 3).

Prespecified sensitivity analyses excluding patients with SPMS did not significantly alter the overall results or impact individual variables.

DISCUSSION

Here, we aimed to longitudinally investigate the association between PRLs and the degree of inner retinal layer thinning in MS. Two main findings emerge from our study: (i) the number of PRLs is associated with subsequent inner retinal layer thinning and (ii) PRLs alone or in a combination with inner retinal layer thinning are associated with an up to eightfold increased risk of PIRA in the following 5 years.

In the past decade, PRLs have gained particular interest as a new imaging biomarker of chronic active MS, often referred to as the "smoldering" disease. PRLs appear to be highly neurodestructive by featuring chronic inflammation with remyelination failure, leading to pronounced myelin loss and axonal degeneration within and around the PRLs [33, 34]. They have been shown to be typically larger than the remaining lesions and to expand slowly over time [1], losing their iron rim and ceasing to expand in the process [7]. Their presence is associated with a more severe disease course [35], higher serum neurofilament light chain levels [36, 37], and faster brain atrophy rates [35, 36]. The characteristics of PRLs were initially studied on

TABLE 2 Multivariate linear regression models.

	aLpRNFL			aLGCIPL		
	β	95% CI	p	β	95% CI	p
PRLs	−0.36	−0.32, −0.26	**<0.001**	−0.50	−0.31, −0.27	**<0.001**
Age	0.24	0.03, 0.04	**<0.001**	0.07	0.01, 0.01	**0.003**
Sex	0.08	0.13, 0.40	**<0.001**	0.04	0.01, 0.18	**0.039**
Disease duration	0.13	0.02, 0.04	**<0.001**	0.06	0.01, 0.02	**0.009**
EDSS at baseline	−0.10	−0.16, −0.05	**<0.001**	−0.16	−0.15, −0.09	**<0.001**
DMT group	0.06	0.04, 0.23	**0.005**	0.05	0.02, 0.15	**0.008**
T2 lesion count	−0.05	−0.01, 0.00	0.065	0.05	0.00, 0.01	0.102
Visual pathway lesion count	0.05	−0.01, 0.05	0.142	−0.03	−0.03, 0.01	0.330
	$\Delta R^2 = 0.100, p < 0.001$			$\Delta R^2 = 0.293, p < 0.001$		

Note: Bold values denote a significant association between PRLs and inner retinal layer thinning, along with other covariates included in the model.
Abbreviations: aLGCIPL, annualized loss of ganglion cell–inner plexiform layer; aLpRNFL, annualized loss of peripapillary retinal nerve fiber layer; CI, confidence interval; DMT, disease-modifying therapy; EDSS, Expanded Disability Status Scale; PRL, paramagnetic rim lesion.

FIGURE 2 Association between the number of paramagnetic rim lesion (PRLs) and annualized loss of peripapillary retinal nerve fiber layer (aLpRNFL; a) and annualized loss of ganglion cell–inner plexiform layer (aLGCIPL; b). CI, confidence interval.

(a) $\beta = -0.36$ (95% CI −0.32, −0.26) $p < 0.001$

(b) $\beta = -0.50$ (95% CI −0.31, −0.27) $p < 0.001$
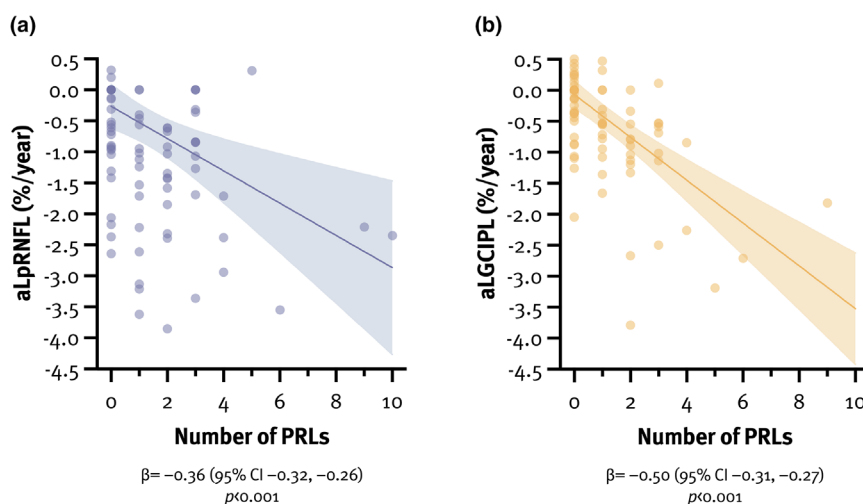
7-T MRI [31], but can also be reliably detected on 3-T and even 1.5-T MRI [38], making them a useful biomarker of chronic active MS, potentially even for routine clinical use.

Here, we show that PRLs likely lead to faster inner retinal layer thinning, a dynamic process that appears to be age-dependent, with faster rates occurring in younger patients [39], which indicates that the period of greatest adaptive immune-mediated inflammatory activity is also the period of the greatest neuroaxonal loss. As subclinical neuroaxonal loss appears to occur early in MS due to residual neuroaxonal reserve [40], the prognostic value of PRL is likely highest early in the disease course (PRLs can be already found in up to 50% of patients with clinically isolated syndrome (CIS)) to stratify patients at higher risk of disability progression, which is the critical determinant of long-term prognosis in MS.

Although the pathophysiology underlying inner retinal layer thinning in MS is not entirely clear, the currently prevailing concept involves retrograde (Wallerian) degeneration secondary to axonal damage occurring anywhere in the brain [41]. Although it was previously thought that only lesions in the visual pathway contribute to inner retinal layer thinning, we show that PRLs, regardless of their

location in the CNS, are also associated with the former, which is consistent with our recent study showing that PRLs lead to pronounced periplaque white matter damage [8]. Thus, changes in the periplaque white matter, or even potentially normal-appearing white matter of patients with PRLs, may contribute to increased inflammatory-driven neuroaxonal loss, reflected by faster inner retinal layer thinning, and thus drive the irreversible disability progression.

This is particularly important because the classic dichotomous division of clinical phenotypes into relapsing and (secondary) progressive MS has recently been challenged, and the currently widely accepted concept is that the clinical course of MS is part of a continuum in which inflammatory activity predominates in the early stages of the disease but can also occur in the later stages and vice versa (smoldering disease). Recent studies have confirmed that disability progression can be observed even in patients with relapsing MS without clinical relapses (PIRA) [42, 43]. This progression, sometimes ill-suitedly termed "silent," occurs in approximately 5% of patients with relapsing MS per year, accounts for at least 50% of all disability accrual events in MS [44], and is reflected in faster brain and spinal cord atrophy rates [9] as well as retinal layer thinning [15],

TABLE 3 Multivariate Cox proportional hazard regression models for risk of progression independent of relapse activity.

Factor	HR	95% CI	p
PRLs (per lesion)	1.24	1.17–1.32	**<0.001**
≥4 PRLs	5.75	4.12–8.03	**<0.001**
aLpRNFL (per %/year)	1.44	1.34–1.56	**<0.001**
aLpRNFL ≥ 1.0%/year	2.59	2.07–3.24	**<0.001**
aLpRNFL ≥ 1.0%/year and ≥4 PRLs	4.70	3.51–6.29	**<0.001**
aLGCIPL (per %/year)	1.61	1.47–1.77	**<0.001**
aLGCIPL ≥ 1.0%/year	2.01	1.60–2.53	**<0.001**
aLGCIPL ≥ 1.0%/year and ≥4 PRLs	8.06	6.11–10.64	**<0.001**
Age (per year)	1.05	1.04–1.07	**<0.001**
Sex	0.88	0.68–1.14	0.320
Disease duration (per year)	1.08	1.05–1.10	**<0.001**
EDSS at baseline (per point)	1.14	1.02–1.29	**0.025**
DMT group (reference: no DMT)			
M-DMT	0.92	0.56–1.54	0.760
H-DMT	2.54	1.60–4.03	**<0.001**
T2 lesion count (per lesion)	1.02	1.02–1.03	**<0.001**
Visual pathway lesion count (per lesion)	1.16	1.12–1.21	**<0.001**

Note: Bold values denote a significant association between PRLs, inner retinal layer thinning and increased likelihood of PIRA, along with other covariates included in the model.

Abbreviations: aLGCIPL, annualized loss of ganglion cell–inner plexiform layer; aLpRNFL, annualized loss of peripapillary retinal nerve fiber layer; CI, confidence interval; DMT, disease-modifying therapy; EDSS, Expanded Disability Status Scale; H-DMT, highly effective DMT; HR, hazard ratio; M-DMT, moderately effective DMT; PRL, paramagnetic rim lesion.

suggesting that neurodegenerative processes may start much earlier than previously thought [22].

In line with this, we show that PRLs are also associated with an increased risk of PIRA, most likely as a result of the aforementioned dynamic changes in PRLs and their surrounding white matter, which may be the ultimate driver of disability accrual. In our study, a combination of both inner retinal layer thinning and the presence of ≥4 PRLs was associated with an up to eightfold increased risk of PIRA, providing a promising stratification tool for future clinical trials to identify patients who may benefit most from tailored therapeutic regimens.

Some limitations of this study must be acknowledged. First, the sample size was relatively small, and the retrospective study design introduced a number of potential biases, although these were mitigated by the detailed and standardized characterization of patients within the VMSD [18]. Thus, replication of our data in an independent cohort is needed for confirmation. Second, the effect of DMT on inner retinal layer thinning was grouped into M-DMT and H-DMT, as the available sample size was insufficient to allow further

subgroup analyses. Third, OCT scans were performed at slightly irregular intervals, which was partially overcome by calculating aLpRNFL and aLGCIPL using linear regression models. In addition, as retinal layer atrophy, similar to brain atrophy, is not specific for MS and may be caused by other conditions such as diabetic maculopathy or compressive optic neuropathy, the applicability of the results is limited to the population without any confounding comorbidities. Finally, some patients had a relatively short clinical follow-up, and PIRA was detected in only 18.6% of patients, limiting complex statistical analysis.

In conclusion, we found that PRLs are associated with faster inner retinal layer thinning in MS, providing additional evidence that patients with PRLs are exposed to a more extensive neurodegenerative process. Thus, we emphasize the importance of early identification of risk for PIRA by a combination of paraclinical biomarkers to prevent irreversible tissue loss and to stratify patients who could benefit most from neuroprotective agents.

AUTHOR CONTRIBUTIONS

CONFLICT OF INTEREST STATEMENT

DATA AVAILABILITY STATEMENT

Data supporting the findings of this study are available from the corresponding author upon reasonable request by a qualified researcher and upon approval by the data-clearing committee of the Medical University of Vienna.

ORCID

Fabian Föttinger https://orcid.org/0009-0005-7970-5349
Barbara Kornek https://orcid.org/0000-0002-1851-6967
Paulus Rommer https://orcid.org/0000-0001-5209-6647
Lukas Haider https://orcid.org/0000-0002-1556-1770
Gabriel Bsteh https://orcid.org/0000-0002-0825-0851

REFERENCES

1. Dal-Bianco A, Grabner G, Kronnerwetter C, et al. Slow expansion of multiple sclerosis iron rim lesions: pathology and 7 T magnetic resonance imaging. *Acta Neuropathol*. 2017;133(1):25-42.
2. Kaunzner UW, Kang Y, Zhang S, et al. Quantitative susceptibility mapping identifies inflammation in a subset of chronic multiple sclerosis lesions. *Brain*. 2019;142(1):133-145.
3. AlTokhis AI, AlOtaibi AM, Felmban GA, Constantinescu CS, Evangelou N. Iron rims as an imaging biomarker in MS: a systematic mapping review. *Diagnostics (Basel)*. 2020;10(11):968.
4. Absinta M, Dal-Bianco A. Slowly expanding lesions are a marker of progressive MS – yes. *Mult Scler*. 2021;27(11):1679-1681.
5. Hofmann A, Krajnc N, Dal-Bianco A, et al. Myeloid cell iron uptake pathways and paramagnetic rim formation in multiple sclerosis. *Acta Neuropathol*. 2023;146:707-724.
6. Absinta M, Sati P, Schindler M, et al. Persistent 7-tesla phase rim predicts poor outcome in new multiple sclerosis patient lesions. *J Clin Invest*. 2016;126(7):2597-2609.
7. Dal-Bianco A, Grabner G, Kronnerwetter C, et al. Long-term evolution of multiple sclerosis iron rim lesions in 7 T MRI. *Brain*. 2021;144:833-847.
8. Krajnc N, Schmidbauer V, Leinkauf J, et al. Paramagnetic rim lesions lead to pronounced diffuse periplaque white matter damage in multiple sclerosis. *Mult Scler*. 2023;29(11–12):1406-1417.
9. Cagol A, Benkert P, Melie-Garcia L, et al. Association of spinal cord atrophy and brain paramagnetic rim lesions with progression independent of relapse activity in people with MS. *Neurology*. 2024;102(1):e207768.
10. Britze J, Frederiksen JL. Optical coherence tomography in multiple sclerosis. *Eye (Lond)*. 2018;32(5):884-888.
11. Saidha S, Sotirchos ES, Oh J, et al. Relationships between retinal axonal and neuronal measures and global central nervous system pathology in multiple sclerosis. *JAMA Neurol*. 2013;70(1):34-43.
12. Bsteh G, Berek K, Hegen H, et al. Macular ganglion cell-inner plexiform layer thinning as a biomarker of disability progression in relapsing multiple sclerosis. *Mult Scler*. 2021;27(5):684-694.
13. Bsteh G, Hegen H, Teuchner B, et al. Peripapillary retinal nerve fibre layer as measured by optical coherence tomography is a prognostic biomarker not only for physical but also for cognitive disability progression in multiple sclerosis. *Mult Scler*. 2019;25(2):196-203.
14. Schurz N, Sariaslani L, Altmann P, et al. Evaluation of retinal layer thickness parameters as biomarkers in a real-world multiple sclerosis cohort. *Eye Brain*. 2021;13:59-69.
15. Bsteh G, Hegen H, Altmann P, et al. Retinal layer thinning is reflecting disability progression independent of relapse activity in multiple sclerosis. *Mult Scler J Exp Transl Clin*. 2020;6(4):2055217320966344.
16. Krajnc N, Dal-Bianco A, Leutmezer F, et al. Association of paramagnetic rim lesions and retinal layer thickness in patients with multiple sclerosis. *Mult Scler*. 2022;29:374-384.
17. Thompson AJ, Banwell BL, Barkhof F, et al. Diagnosis of multiple sclerosis: 2017 revisions of the McDonald criteria. *Lancet Neurol*. 2018;17(2):162-173.
18. Bsteh G, Hegen H, Riedl K, et al. Quantifying the risk of disease reactivation after interferon and glatiramer acetate discontinuation in multiple sclerosis: the VIAADISC score. *Eur J Neurol*. 2021;28(5):1609-1616.
19. Bsteh G, Hegen H, Krajnc N, et al. Retinal layer thinning for monitoring disease modifying treatment in relapsing multiple sclerosis – evidence for applying a rebaselining concept (MSMilan2023 – Oral presentations). *Mult Scler J*. 2023;29(3_suppl):4-136.
20. Kurtzke JF. Rating neurologic impairment in multiple sclerosis: an expanded disability status scale (EDSS). *Neurology*. 1983;33(11):1444-1452.
21. Poser CM, Paty DW, Scheinberg L, et al. New diagnostic criteria for multiple sclerosis: guidelines for research protocols. *Ann Neurol*. 1983;13(3):227-231.
22. Kappos L, Wolinsky JS, Giovannoni G, et al. Contribution of relapse-independent progression vs relapse-associated worsening to overall confirmed disability accumulation in typical relapsing multiple sclerosis in a pooled analysis of 2 randomized clinical trials. *JAMA Neurol*. 2020;77(9):1132-1140.

23. Kappos L, Butzkueven H, Wiendl H, et al. Greater sensitivity to multiple sclerosis disability worsening and progression events using a roving versus a fixed reference value in a prospective cohort study. *Mult Scler.* 2018;24(7):963-973.

24. Pemp B, Kardon RH, Kircher K, Pernicka E, Schmidt-Erfurth U, Reitner A. Effectiveness of averaging strategies to reduce variance in retinal nerve fibre layer thickness measurements using spectral-domain optical coherence tomography. *Graefes Arch Clin Exp Ophthalmol.* 2013;251(7):1841-1848.

25. Classification of Diabetic Retinopathy from Fluorescein Angiograms. ETDRS report number 11. Early Treatment Diabetic Retinopathy Study Research Group. *Ophthalmology.* 1991;98(5 Suppl):807-822.

26. Tewarie P, Balk L, Costello F, et al. The OSCAR-IB consensus criteria for retinal OCT quality assessment. *PLoS One.* 2012;7(4):e34823.

27. Nolan-Kenney RC, Liu M, Akhand O, et al. Optimal intereye difference thresholds by optical coherence tomography in multiple sclerosis: an international study. *Ann Neurol.* 2019;85(5):618-629.

28. Bsteh G, Hegen H, Altmann P, et al. Validation of inter-eye difference thresholds in optical coherence tomography for identification of optic neuritis in multiple sclerosis. *Mult Scler Relat Disord.* 2020;45:102403.

29. Saidha S, Al-Louzi O, Ratchford JN, et al. Optical coherence tomography reflects brain atrophy in multiple sclerosis: a four-year study. *Ann Neurol.* 2015;78(5):801-813.

30. Aytulun A, Cruz-Herranz A, Aktas O, et al. APOSTEL 2.0 recommendations for reporting quantitative optical coherence tomography studies. *Neurology.* 2021;97(2):68-79.

31. Absinta M, Sati P, Masuzzo F, et al. Association of chronic active multiple sclerosis lesions with disability in vivo. *JAMA Neurol.* 2019;76(12):1474-1483.

32. Council National Research. *The Prevention and Treatment of Missing Data in Clinical Trials.* 2010. USA: National Academies Press.

33. Kornek B, Storch MK, Weissert R, et al. Multiple sclerosis and chronic autoimmune encephalomyelitis: a comparative quantitative study of axonal injury in active, inactive, and remyelinated lesions. *Am J Pathol.* 2000;157(1):267-276.

34. Bramow S, Frischer JM, Lassmann H, et al. Demyelination versus remyelination in progressive multiple sclerosis. *Brain.* 2010;133(10):2983-2998.

35. Absinta M, Sati P, Masuzzo F, et al. Association of chronic active multiple sclerosis lesions with disability in vivo. *JAMA Neurol.* 2019;76:1474–1483.

36. Dal-Bianco A, Schranzer R, Grabner G, et al. Iron rims in MS patients as neurodegenerative marker? – a 7 Tesla Magnetic Resonance Study. *Front Neurol.* 2021;12:632749.

37. Maggi P, Kuhle J, Schadelin S, et al. Chronic white matter inflammation and serum neurofilament levels in multiple sclerosis. *Neurology.* 2021;97(6):e543-e553.

38. Hemond CC, Reich DS, Dundamadappa SK. Paramagnetic rim lesions in multiple sclerosis: comparison of visualization at 1.5-T and 3-T MRI. *AJR Am J Roentgenol.* 2022;219(1):120-131.

39. Cordano C, Nourbakhsh B, Yiu HH, et al. Differences in age-related retinal and cortical atrophy rates in multiple sclerosis. *Neurology.* 2022;99:e1685-e1693.

40. Balk LJ, Cruz-Herranz A, Albrecht P, et al. Timing of retinal neuronal and axonal loss in MS: a longitudinal OCT study. *J Neurol.* 2016;263(7):1323-1331.

41. Dinkin M. Trans-synaptic retrograde degeneration in the human visual system: slow, silent, and real. *Curr Neurol Neurosci Rep.* 2017;17(2):16.

42. Dekker I, Leurs CE, Hagens MHJ, et al. Long-term disease activity and disability progression in relapsing-remitting multiple sclerosis patients on natalizumab. *Mult Scler Relat Disord.* 2019;33:82-87.

43. University of California SFMSET, Cree BAC, Hollenbach JA, et al. Silent progression in disease activity-free relapsing multiple sclerosis. *Ann Neurol.* 2019;85(5):653-666.

44. Muller J, Cagol A, Lorscheider J, et al. Harmonizing definitions for progression independent of relapse activity in multiple sclerosis: a systematic review. *JAMA Neurol.* 2023;80(11):1232-1245.

SUPPORTING INFORMATION

Additional supporting information can be found online in the Supporting Information section at the end of this article.